Impact of quantum–classical correspondence on entanglement enhancement by single-mode squeezing

Sijo K. Joseph [a], Lock Yue Chew [b], Miguel A.F. Sanjuán [a],*

[a] *Nonlinear Dynamics, Chaos and Complex Systems Group, Departamento de Física, Universidad Rey Juan Carlos, Tulipán s/n, 28933 Móstoles, Madrid, Spain*
[b] *Division of Physics and Applied Physics, School of Physical and Mathematical Sciences, Nanyang Technological University, 21 Nanyang Link, 637371 Singapore*

ARTICLE INFO

ABSTRACT

Quantum entanglement between two field modes can be achieved through the collective squeezing of the two respective modes. If single-mode squeezing is performed prior to such a two-mode squeezing, an enhancement of entanglement production can happen. Interestingly, the occurrence of this enhancement can be implicitly linked to the local classical dynamical behavior via the paradigm of quantum–classical correspondence. In particular, the entanglement generated through quantum chaos is found to be hardly enhanced by prior squeezing, since it is bounded by the saturation value of the maximally entangled Schmidt state with fixed energy. These results illustrate that entanglement enhancement via initial squeezing can serve as a useful indicator of quantum chaotic behaviour.

1. Introduction

In the last decades, a number of quantum information protocols which utilizes continuous-variable (CV) entanglement have been developed [2,6,44]. The performance of these protocols is often constrained by the achievable degree of the entanglement that is being produced. In particular, a stable control of entanglement generation is necessary before quantum cryptography with a finite number of samples can be secured against the most general coherent attacks [15]. It is noteworthy that while various schemes of generating controllable CV entanglement have been proposed, a major scheme of interest is that of two-mode squeezing. In fact, it has been shown via diverse quantum systems that the generation of entanglement can be enhanced by performing single-mode squeezing prior to two-mode squeezing. In the Jaynes–Cummings model for example, it has been demonstrated that a stronger entanglement between a two-level atom and an electromagnetic field mode can be achieved by using a squeezed state rather than a coherent state as the initial photon state [16]. Note that in this case the enhancement is observed only when the initial state of the field mode is sufficiently squeezed. Similar threshold has also been observed in systems of coupled harmonic oscillators [13]. Beyond the threshold, the maximum attainable entanglement is found to grow steadily with an increase in the initial squeezing parameter. In another interesting investigation, the enhancement in entangle-

ment via unequal single-mode squeezing performed separately on the two field modes was studied [40]. Notably, entanglement was found to persist even in a decohering environment with high temperature when the normal modes are squeezed [18].

Experimental schemes for generating CV entanglement was first proposed and realized in non-degenerate parametric amplifiers [38,47]. Later, non-degenerate three-level cascade laser was suggested as an alternative optical system for the experimental generation of entangled quantum state. For this setup, an enhancement of intra-cavity quadrature squeezing was observed by coupling the cavity mode to a squeezed vacuum reservoir. The effect of the squeezed vacuum was studied and the result is a large enhancement of the intra-cavity squeezing and entanglement in the two-mode light [1]. Further investigations on this topic were focused on the search for effective ways to increase the initial single-mode squeezing with easily implementable schemes that can generate a high degree of squeezing and entanglement. On the other hand, our interest is to examine into new schemes which could exploit the effectiveness of initial single-mode squeezing on entanglement enhancement beyond the control of the amplitude and orientation of prior squeezing or the existence of a critical squeezing parameter. A particular novel idea is to employ the fundamental physics of quantum-to-classical correspondence to guide the process of entanglement enhancement with initial squeezing through the perspective of classical dynamics. The potential effectiveness of this new approach would be surprising and counter-intuitive since both squeezing and entanglement are purely quantum phenomena.

Indeed, the correspondence between the physics of quantum systems and its classical counterparts has been well-established for

* Corresponding author.
E-mail addresses: sijo.joseph@urjc.es (S.K. Joseph), lockyue@ntu.edu.sg (L.Y. Chew), miguel.sanjuan@urjc.es (M.A.F. Sanjuán).

decades [5,17,33,42]. Notable examples include the manifestation of chaos in the energy-level distribution [42] of atomic systems, as well as the wave patterns that are exhibited in quantum chaotic systems which are known as 'scars' [5]. In recent years, there has been an increasing interest in correlating the entanglement production of a quantum system with the corresponding dynamical behaviour in the classical domain. For example, the dynamical production of entanglement was studied on the N-atoms Jaynes–Cummings model [17] for initial coherent states whose centers lie in different regions of the corresponding classical phase space. The entanglement production was found to be a good indicator of the regular-to-chaotic transition that happens in the classical domain. Similar studies were undertaken for kicked tops [3,4,8,14,31,34], the 4D standard maps [28], nonlinear oscillators [10,46], the Dicke model [41], Rydberg molecule [30], triatomic molecules [24,45], integrable dimers [23] and interacting spins [35]. In this paper, we shall show the effectiveness of entanglement enhancement through initial squeezing, and more importantly, demonstrate its dependence on the local dynamical behavior of the corresponding classical phase space. Interestingly, for initial coherent states whose centers lie in the regular regimes of the classical phase space, the maximum attainable entanglement can be enhanced significantly by performing prior single-mode squeezing. In addition, the amount of entanglement enhancement is found to increase monotonically with the degree of prior squeezing. Conversely, for initial coherent states whose centers lie in chaotic regions of the classical phase space, prior single-mode squeezing is observed to have negligible effects in enhancing the quantum entanglement.

2. Model

In this study, we consider bipartite system composed of two coupled anharmonic oscillators [9,11,37]. Specifically, we focus on the following Hamiltonian:

$$H = \frac{p_1^2}{2} + \frac{p_2^2}{2} + \frac{1}{2}q_1^2 + \frac{1}{2}q_2^2 + \lambda q_1^2 q_2^2. \tag{1}$$

In the equation, p_1 and p_2 denote the kinetic momenta, while q_1 and q_2 denote the oscillators' positions, with λ being the coupling parameter. The classical dynamics of this model has been shown to range from regular, to mixed regular, and chaotic [37]. Upon quantization, the corresponding dynamical production of entanglement with initial separable coherent states was found to relate closely to the classical trajectories [46]. Specifically, the maximum value of the entanglement production is found to correspond systematically to the classical invariant tori and is the largest when the initial state lies at the edge of the regular islands or in the chaotic sea.

The initial state is chosen to be a tensor product of the coherent state, $|\psi(0)\rangle = |\alpha_1\rangle \otimes |\alpha_2\rangle$, whose center lies precisely on a classical phase point (q_1, p_1, q_2, p_2) with $\alpha_k = (q_k + ip_k)/\sqrt{2}$, where $k = 1, 2$. In other words, the classical phase point (q_1, p_1, q_2, p_2) gives the center of the initial coherent state. Prior to the dynamical generation of entanglement through the Hamiltonian given by Eq. (1), single-mode squeezing is performed individually on each subsystem initial state by the following squeezing operator:

$$\hat{S}(\zeta_k) = e^{\frac{1}{2}\zeta_k^* \hat{a}_k^{\dagger 2} - \frac{1}{2}\zeta_k \hat{a}_k^2}. \tag{2}$$

The result is a product state of single-mode squeezed coherent state: $|\psi(0)\rangle = |\alpha_1, \zeta_1\rangle \otimes |\alpha_2, \zeta_2\rangle$ where

$$|\alpha_k, \zeta_k\rangle = \hat{S}(\zeta_k)|\alpha_k\rangle, \tag{3}$$

with $k = 1, 2$. Note that $\hat{a}_k = (\hat{q}_k + i\hat{p}_k)/\sqrt{2}$, with $\hat{q}_k$ and $\hat{p}_k$ being the position and momentum operators respectively. Also, $\zeta_k = |\zeta_k|\exp(i2\theta_k)$ denotes the squeezing parameter for mode k which quantifies the degree of single-mode squeezing.

The time evolution of the quantum state $|\psi(t)\rangle$ is given by

$$|\psi(t)\rangle = \hat{U}(t)|\psi(0)\rangle, \tag{4}$$

where the time evolution operator $\hat{U}(t)$ is given by $\hat{U}(t) = e^{-i\hat{H}t/\hbar}$, with $\hat{H}$ being the quantized Hamiltonian:

$$\hat{H} = \left(\hat{a}_1^\dagger \hat{a}_1 + \frac{1}{2}\right) + \left(\hat{a}_2^\dagger \hat{a}_2 + \frac{1}{2}\right) + \frac{\lambda}{4}\left(\hat{a}_1^\dagger + \hat{a}_1\right)^2 \left(\hat{a}_2^\dagger + \hat{a}_2\right)^2 \tag{5}$$

of Eq. (1). The time evolved density matrix is then determined as follow:

$$\rho(t) = \hat{U}(t)\rho(0)\hat{U}(t)^\dagger, \tag{6}$$

where $\rho(0) = |\psi(0)\rangle\langle\psi(0)|$. By taking the partial trace of $\rho(t)$ over the l-th subsystem, the reduced density matrix $\rho_l(t)$ is obtained. The von Neumann entropy of entanglement $S_{vn}(t)$ is then evaluated via

$$S_{vn}(t) = -\text{Tr}\left[\rho_l(t)\log_2\rho_l(t)\right] = -\sum_{i=1}^{N}\lambda_i\log_2\lambda_i, \tag{7}$$

where $l = 1$ or 2 and N is the basis size employed in the numerical simulation.

3. Effect of squeezing on entanglement enhancement

To probe the dependence on local classical dynamics, we consider specifically the effect of prior single-mode squeezing on entanglement enhancement for the situation when the classical phase space exhibits both a mixture of regular and chaotic behaviour. For this, the energy $E = 150.75$ and the coupling constant $\lambda = 0.0075$ is selected. The Poincaré surface is shown in Fig. 1 where we observe groups of regular islands within a sea of chaos. Specifically, the dynamics displayed by the trajectories of this system is very different depending on the initial condition. While a regular orbit is restricted within a small region of the regular tori, the temporal position of a chaotic trajectory spreads out unpredictably within the chaotic sea. In Fig. 2, we show entanglement dynamics of four initial coherent states with centers lie at different positions of this classical mixed phase space. For each coherent state, a single-mode squeezing is performed on both the oscillator field modes (with $\zeta_1 = \zeta_2 = \zeta$) before the dynamical generation of quantum entanglement. Interestingly, the enhancement of entanglement production is not uniform for the four chosen initial coherent states although each of them is subjected to the same amplitude of single-mode squeezing prior to two-mode squeezing which generates entanglement. In particular, entanglement production is found to be higher for initial states with centers lie in the chaotic region compared to the regular region. When equal amount of prior single-mode squeezing are performed on the initial states, enhancement of entanglement is found to be larger for quantization of the regular orbit versus that of the chaotic orbit (see Fig. 2). In addition, we found that entanglement can be effectively enhanced when a higher degree of single-mode squeezing is injected prior to the dynamical generation of entanglement as shown in Fig. 3. However, prior squeezing has minimal enhancement effect on entanglement generation when the center of the initial state lies in the chaotic regime of the classical counterpart. Note that similar results are obtained for numerical computation performed for prior squeezing with different angles ($\theta = \pi/4, \pi/2$ and $3\pi/4$).

4. Dependence of entanglement enhancement on local classical dynamical behaviour

While the correspondence between the quantum system and its classical counterpart has been witnessed in various contexts,
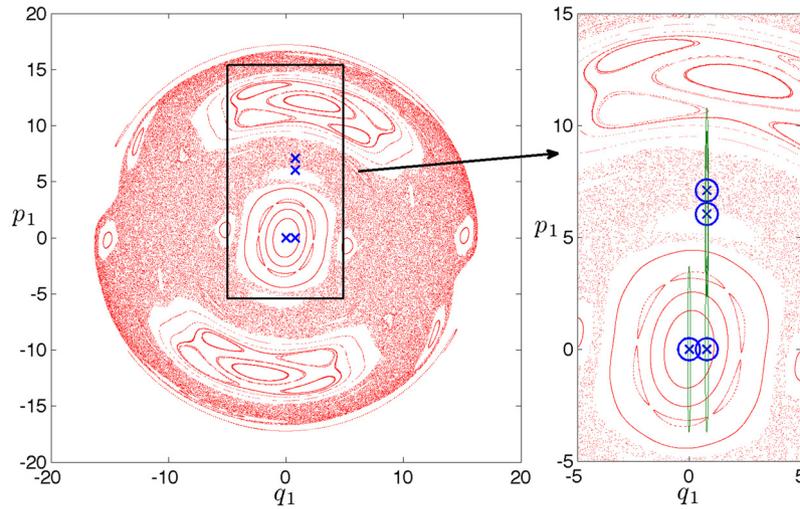
Fig. 1. A plot of the Poincaré section of the classical mixed phase space on the q_1–p_1 plane with $q_2 = \sqrt{5}$ and $p_2 > 0$. The parameters used are $E = 150.75$ and $\lambda = 0.0075$. The cross markers show the initial conditions chosen to study the entanglement dynamics. They represent the centers of the initial coherent states: $(q_1, p_1) = (0, 0)$, $(q_1, p_1) = (\sqrt{10}/4, 0)$, $(q_1, p_1) = (\sqrt{10}/4, 1.9102\sqrt{10})$ and $(q_1, p_1) = (\sqrt{10}/4, 2.2427\sqrt{10})$ employed in our numerical simulations. In addition, they are the initial conditions that lead to the subplots (a), (b), (c) and (d) respectively in the subsequent figures. Note that the inset show the variance ellipses for the squeezed (green ellipse) and non-squeezed (blue circle) case to illustrate the size of the initial wave packet. (For interpretation of the references to color in this figure legend, the reader is referred to the web version of this article.)
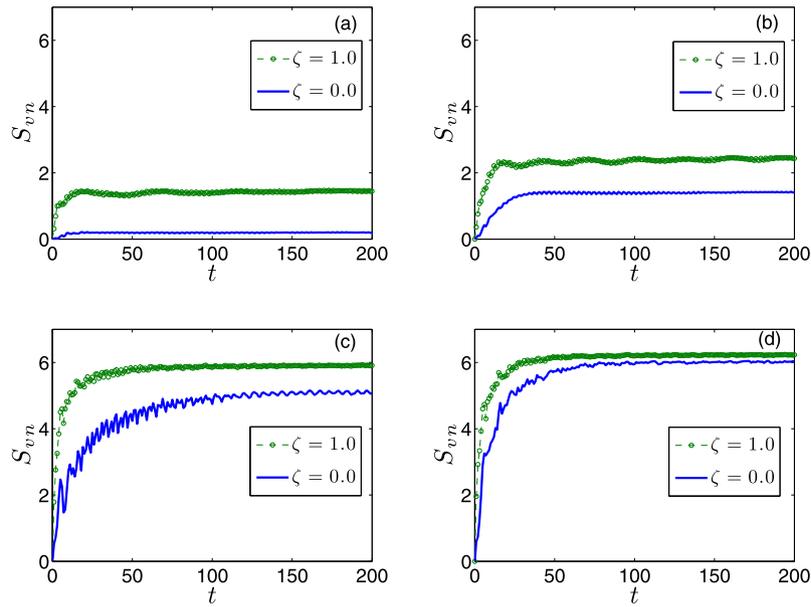
Fig. 2. Entanglement dynamics for initial coherent states with centers sampled from different parts of the classical mixed phase space shown in Fig. 1. The classical dynamics are: (a) regular, (b) regular, (c) at the edge of regular and chaotic regimes, and (d) chaotic. Solid lines show entanglement dynamics for initial coherent states without prior single-mode squeezing while dashed lines with circles show entanglement dynamics for initial coherent states subjected to prior single-mode squeezing with $\zeta_1 = \zeta_2 = \zeta = 1$.

this is the first illustration of its manifestation via the effect of initial squeezing on entanglement enhancement. Indeed, such enhancement can be a good indicator of regular-to-chaotic transition in the mixed phase space regime. Specifically, while the generation of entanglement is insensitive to the squeezing of initial states whose center lie in the chaotic region of the mixed phase space, the squeezing of initial states whose center lie in the regular part has a positive impact on the enhancement of entanglement. This observation can be discerned through a detailed numerical analysis based on the quantum density spectrum as shown in Fig. 4, which is obtained by yielding the diagonal elements of the density matrix of the coupled system evaluated at the eigenstates of the Hamiltonian given by Eq. (1) [46]. In fact, the calculation of the quantum density spectrum can also be performed by taking the Fourier transform of the autocorrelation $\langle \psi(t) | \psi(0) \rangle$, which is more effi-

cient. The upshot is that the degree of entanglement of the system is closely related to the number of significant components of the quantum density spectrum. Indeed, we observe that the quantum states which correspond to the chaotic regime possess more spectral elements (Fig. 4(d)) and have a larger entanglement relative to that of the regular regime (Fig. 4(a) or 4(b)). More importantly, we uncovered that the inclusion of initial squeezing has the effect of increasing the number of components in the quantum density spectrum, as depicted in Figs. 4(e) to 4(f). The increase is larger for the regular case and the case that borders between regularity and chaos than the chaotic case, which is consistent with our earlier result that a larger entanglement enhancement occurs within the regular tori versus that of the chaotic sea.

In the coupled kicked top model, dynamically generated entanglement is found to be bounded by a finite value [3]. In particular,
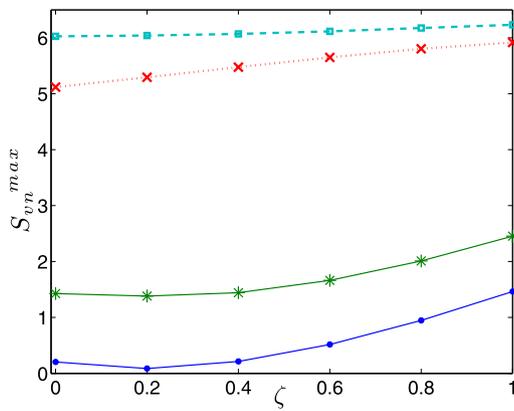
Fig. 3. Dependence of the entanglement entropy at saturation on the amplitude of prior squeezing for the four initial states used in Fig. 2. Here the dot and the star markers denote the regular initial conditions. The cross marker denotes the initial condition selected from the boarder of the chaotic sea and the KAM island. The square markers show the entanglement maxima of the point selected from the middle of the chaotic sea. The parameters employed are $E = 150.75$ and $\lambda = 0.0075$.

Fig. 5. A plot of the entanglement entropy against time t for the classically chaotic orbits. The dashed and dotted curves show the entanglement dynamics of the chaotic initial condition with ($\zeta_1 = \zeta_2 = \zeta = 1.0$) and without prior single mode squeezing respectively. The upper solid curve illustrates the entanglement dynamics for an initial maximally entangled state with Schmidt mode number $N_m = 108$. Here, the chosen system parameters are: $E = 150.75$ and $\lambda = 0.0075$.

for initial states that lie within the chaotic sea, entanglement production is observed to saturate within a short time. Interestingly, by starting from a maximally entangled initial state, time evolution would partially disentangle the state such that in the long time limit, entanglement would reach the same saturation value. Now, the results in the previous section seem to suggest that entanglement between two oscillators generated by quantum chaos cannot be increased beyond a certain limit by prior squeezing. Here, we shall examine into the 'entanglement bound' by evolving a 'maximally entangled' state:

$$|\psi\rangle = \frac{1}{\sqrt{N_m}} \sum_{m=0}^{N_m-1} |m\rangle^{[1]} \otimes |m\rangle^{[2]}, \tag{8}$$

where $|m\rangle^{[1]}$ and $|m\rangle^{[2]}$ are the one dimensional harmonic oscillator eigenfunctions of subsystem 1 and 2. Note that Eq. (8) takes the form of the Schmidt decomposition of $|\psi\rangle$, and in our case, we need to ensure that the average energy $\langle\psi|\hat{H}|\psi\rangle$ given by this state is close to the energy associated with the chaotic initial condition, which is $E = 150.75$. By means of numerical calculation, the number of Schmidt modes is determined to be $N_m \approx 108$. We next examine the entanglement dynamics with this maximally entangled initial state based on the Hamiltonian given by Eq. (5). As

time increases, we observe that the entanglement entropy reduces from its maximum value to a stationary saturated value as shown in Fig. 5. We shall take this stationary value as the upper bound of the entanglement entropy in accordance with Ref. [3]. We observe that the entanglement entropy for the quantization of classically chaotic trajectory at the steady state is close to this bound. Interestingly, it seems that prior single-mode squeezing is not able to generate entanglement that surpasses this entanglement bound. In consequence, there is no significant enhancement in entanglement generation when prior single-mode squeezing is applied to a coherent state with center lies in the chaotic sea. On the other hand, for quantization of regular orbits, the entanglement entropy is far below the entanglement bound and hence is not constrained by it.

Finally, we explore the quantum-to-classical correspondence by first defining a classical Gaussian ensemble in the four dimensional phase space with a mean value $\mu = (q_1, p_1, q_2, p_2)$ which corresponds to the initial quantum coherent state. Note that a sample of M initial points is considered in this ensemble. Then, the time evolution of the initial ensemble is then calculated using the classical Hamilton equations. On the other hand, for the case with prior squeezing, we shall create a squeezed ensemble of the M samples from the above Gaussian ensemble using the covariance matrix
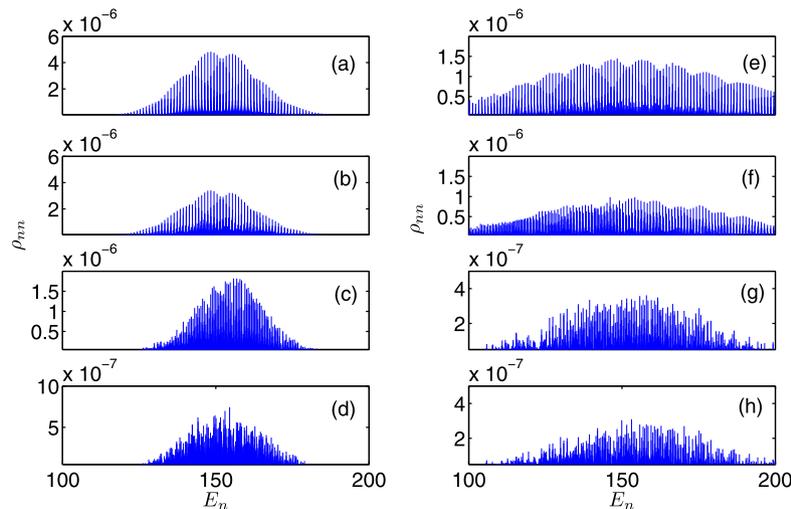
Fig. 4. A plot of the quantum power density spectrum which corresponds to the initial state selected in Fig. 2. The left column is for spectral obtained via initial coherent state and the right column for that determined from initial squeezed coherent state with $\zeta = 1$. The first row (a) and (e) is for regular orbit; the second row (b) and (f) is for another regular orbit; the third row (c) and (g) is for the case at the border of regular and chaotic orbit; while the last row (d) and (h) is for chaotic orbit.
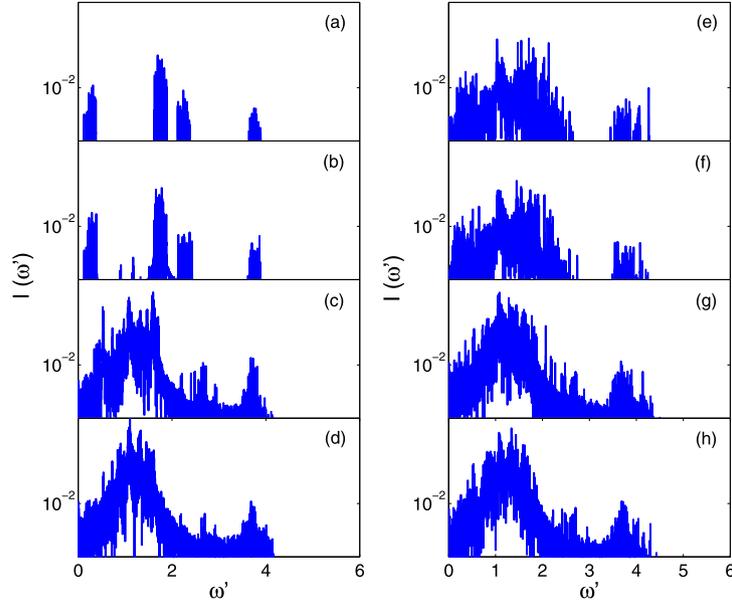
Fig. 6. A plot of the average classical power spectral density which corresponds to the quantum power density spectrum of Fig. 4. Note that both the ensemble size used for the Gaussian and squeezed Gaussian ensemble is 50. The left column is obtained via the initial Gaussian ensemble while the right column from the initial squeezed Gaussian ensemble with $\delta = 2$. The first row (a) and (e) is for regular orbit; the second row (b) and (f) is for another regular orbit; the third row (c) and (g) is for the case at the border of regular and chaotic orbit; while the last row (d) and (h) is for chaotic orbit.
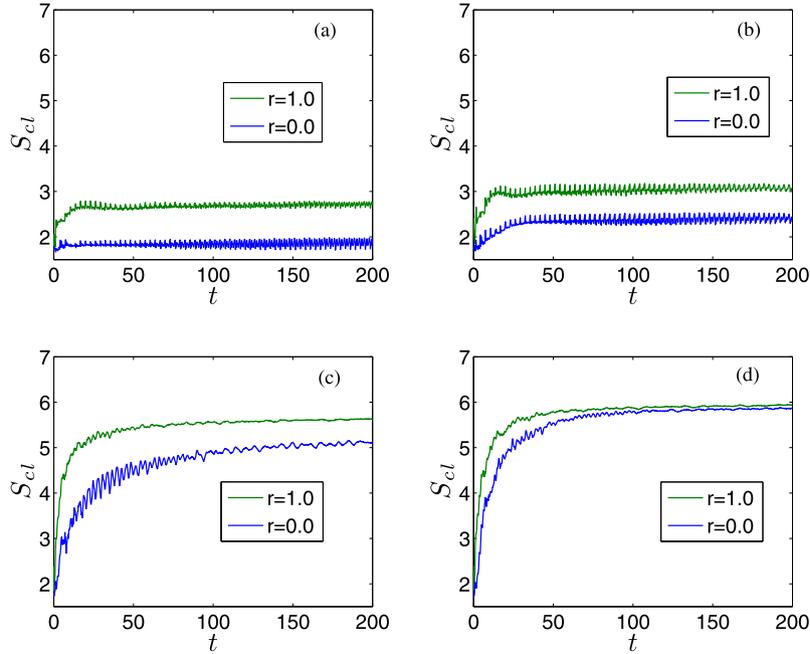
Fig. 7. Dependence of the classical entropy of entanglement at saturation on the amplitude of prior squeezing for the four initial classical distribution which correspond to the quantum state used in Fig. 2. The classical dynamics are: (a) regular, (b) regular, (c) at the edge of regular and chaotic regimes, and (d) chaotic. The parameters employed are $M = 10\,000$, $\delta = 2.0$, $E = 150.75$ and $\lambda = 0.0075$.

$$S_q = \frac{\delta}{4} \begin{bmatrix} \exp(-2r_1) & 0 & 0 & \\ 0 & \exp(2r_1) & 0 & 0 \\ 0 & 0 & \exp(-2r_2) & 0 \\ 0 & 0 & 0 & \exp(2r_2) \end{bmatrix}$$

before subjecting it to time evolution from the Hamilton's equation. Here δ is the classical analog of the Planck constant $\hbar$. r_1 and r_2 is analogous to the squeezing parameter ζ_1 and ζ_2 respectively. For the i-th trajectory $q_1^i(t)$ from either of these ensembles, we compute the classical power spectral density [46]:

$$I_1^i(\omega) = \frac{1}{2\pi} \lim_{T \to \infty} \frac{1}{T} \left| \int_0^T dt\, q_1^i(t) \exp(-i\omega t) \right|^2, \qquad (9)$$

from which we obtain the average classical power spectral density

$$\bar{I}_1(\omega) = \frac{1}{M} \sum_{i=1}^{M} I_1^i(\omega). \qquad (10)$$

A plot of $\bar{I}_1(\omega)$ against ω is given in Fig. 6 where the left column corresponds to the initial Gaussian ensemble while the right column to the squeezed initial Gaussian ensemble. Like the quan-
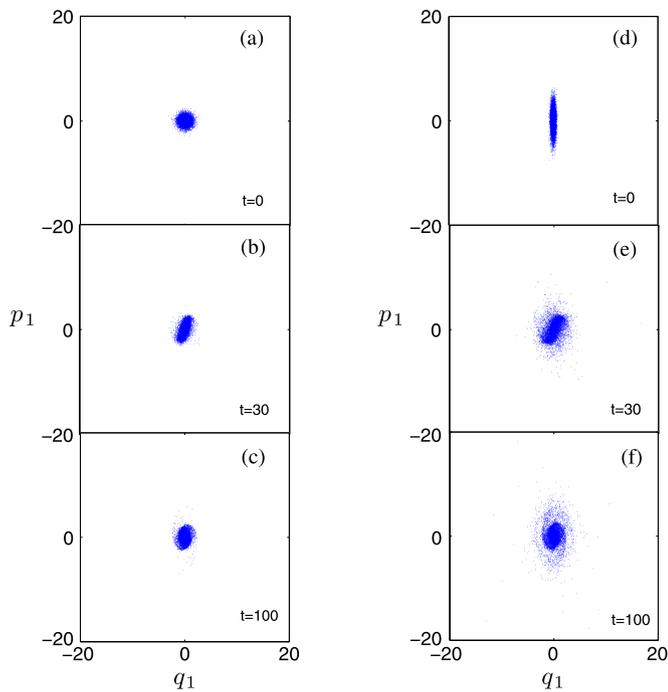
Fig. 8. The time evolution of the classical distribution centered on a regular initial condition is plotted at different instants of time in the projected phase-space q_1–p_1. Figures (a), (b) and (c) show coherent distribution with $r = 0.0$ at time $t = 0$, $t = 30$ and $t = 100$ respectively. On the other hand, figures (d), (e) and (f) illustrate time evolution of a squeezed distribution with $r = 1.0$ at time $t = 0$, $t = 30$ and $t = 100$ respectively. Here, the ensemble size used is $M = 10\,000$ and the parameters employed are $E = 150.75$ and $\lambda = 0.0075$.

Fig. 9. The time evolution of the classical distribution centered on the chaotic initial condition is plotted at different instants of time in the projected phase-space q_1–p_1. Figures (a), (b) and (c) show coherent distribution with $r = 0.0$ at time $t = 0$, $t = 30$ and $t = 100$ respectively. On the other hand, figures (d), (e) and (f) illustrate time evolution of a squeezed distribution with $r = 1.0$ at time $t = 0$, $t = 30$ and $t = 100$ respectively. Here, the ensemble size used is $M = 10\,000$ and the parameters employed are $E = 150.75$ and $\lambda = 0.0075$.

tum density spectrum, the number of significant average classical power spectral density components is larger for initial Gaussian ensemble in the chaotic sea than in the regular tori. In addition, prior squeezing of the Gaussian ensemble has the effect of increasing the number of spectral components, with a larger enhancement for the regular initial states than the chaotic counterparts just like the quantum case.

Next, we plot the classical entropy of entanglement introduced by Casati et al. [7] in Fig. 7. For this, we partition the two-dimensional phase plane q_1–p_1 with square cells of side $\sqrt{\delta}$. The classical entropy is defined as

$$S_{\text{cl}}(\delta, t) = -\sum_i \frac{w_i(t)}{M} \ln \frac{w_i(t)}{M}, \quad (11)$$

where $w_i(t)$ is the number of phase points in the ith cell at time t. Casati et al. [7] had found that this classical entropy would approximate the entropy of the quantum reduced ensemble at the semiclassical limit. In Fig. 7, we have plotted the classical entropy for the squeezed and non-squeezed ensemble for all the four initial states. From the figure, it is obvious that the enhancement in saturation value of the classical entropy is smaller for the chaotic case in comparison to the regular case. This is exactly in accordance with the results based on the von Neumann entropy of entanglement. In addition, we have analyzed the time evolution of classical distributions which correspond to the initial coherent and initial squeezed states. Our results are plotted in Figs. 8 and 9 for the regular and chaotic orbits respectively. The figures show that the phase space region occupied by the distributions increase as time progresses. For the regular orbits as shown in Fig. 8, the phase space region occupied by the evolved distribution is small which is expected from the observed lower value of the classical entropy. Note that Figs. 8(a), (b) and (c) are for initial classical distributions with a non-squeezed ensemble, while Figs. 8(d), (e)
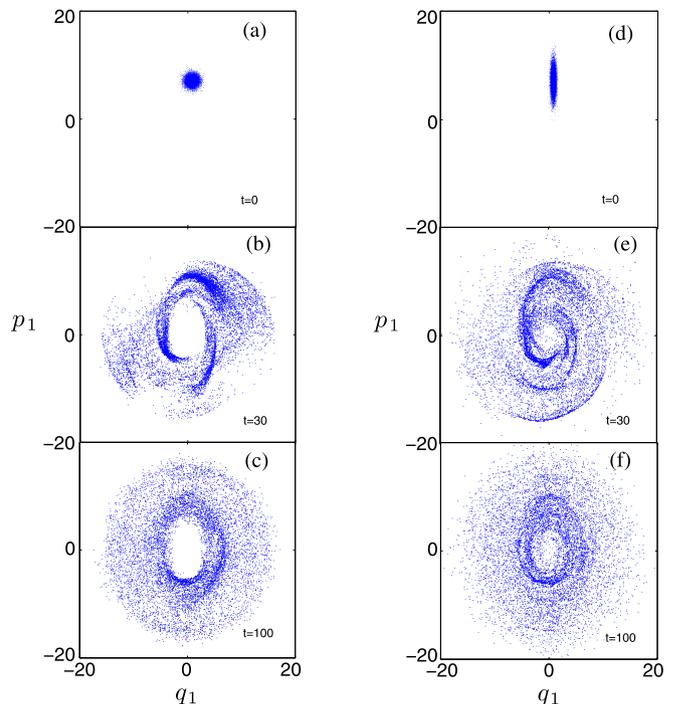
and (f) are for distributions that begin with a squeezed ensemble of $r = 1.0$. Notice that initial squeezing has led to an increase in phase space region accessed by the evolved distribution. On the other hand, Fig. 9 shows that the time evolved distribution of the chaotic orbits occupy a larger phase space which explains its larger entropies. While initial squeezing in this case does increase the accessible region of the phase space as illustrated via Figs. 9(c) and (f), the relative increase is observed to be smaller than that between Figs. 8(c) and (f) for the regular case. This is because the squeezed and non-squeezed ensemble for the chaotic case has already accessed almost all parts of phase space and any increase in accessible regions through squeezing can give only a small contribution. This explains the negligible enhancement of the classical entropy via squeezing for the chaotic initial conditions, and also account for the results displayed in the classical power spectra. In summary, the initial conditions from the squeezed ensemble in the regular domain has led to a sampling of a larger range of regular tori in the phase space than the non-squeezed case. The consequence is the addition of new quasi-periodic frequency components to the average classical power density spectrum. On the other hand, for the chaotic case, trajectories from initial conditions that originate from the squeezed or non-squeezed ensemble are found to sample a very similar chaotic phase space. Thus, we expect a very similar average classical power spectral density with a similar number of frequency components. Since the average classical power spectral density indicates the energy levels that are involved in the corresponding quantum evolution [19,20,46], this explains the analogous results displayed by the quantum density spectrum. With the number of components in the quantum density spectrum being directly related to the amount of entanglement production, our results affirm the idea of quantum–classical correspondence and demonstrates concretely the dependence between

entanglement production and the local classical dynamical behaviour.

5. Conclusion

When single-mode squeezing is injected into the initial separable coherent states prior to the entanglement generation process, it is possible to obtain highly entangled CV quantum states. These highly entangled CV quantum states are resources that are invaluable for the implementation of various quantum protocols employed in quantum cryptography [15] and quantum telecloning [32]. The maximum attainable entanglement depends on both the orientation and amplitude of the prior single-mode squeezing. In this paper, we show that the enhancement of entanglement by prior squeezing can be influenced by the local dynamical behavior of the system's classical counterpart. For initial coherent states whose centers lie in the regular regimes of the classical phase space, the maximum attainable entanglement can be enhanced significantly by performing prior single-mode squeezing. On the other hand, for initial coherent states whose centers lie in chaotic regimes of the classical phase space, prior single-mode squeezing has minimal effects on quantum entanglement enhancement. This result suggests the application of entanglement enhancement via initial squeezing as an indicator of quantum chaotic behaviour. Indeed, in the literature, there are various indicators of quantum chaos, such as the fidelity measure between two quantum states [25,36,12], the Kullback–Leibler quantum divergence [26], and the purity of quantum states [39]. The quantum signature of chaos can also be identified using the universal correspondence between the eigenvalue and eigenvector statistics of quantized classically chaotic system and the canonical ensembles of random matrix theory [21,22,27]. A more visual approach would employ quantum distribution function where the quantum manifestations of classical chaos in phase space can be discerned through the Wigner or the Husimi distribution function [29]. While quantum entanglement has been known to act as a signature of quantum chaos [34,43], the inclusion of initial squeezing has the advantage of detecting local quantum chaotic behaviour without the need to make comparison between the entanglement entropy of the chaotic and regular quantum states. In other words, the detection is performed by probing a quantum chaotic system with an initial coherent and an initial squeezed state, and examining the consequential entanglement enhancement. The magnitude of the enhancement shall indicate whether the quantum chaotic system resides in the regular or chaotic regime. We perceive that our findings here is general and could be applicable to other quantum chaotic systems.

Acknowledgements

References

[1] E. Alebachew, Enhanced squeezing and entanglement in a non-degenerate three-level cascade laser with injected squeezed light, Opt. Commun. 280 (2007) 133.

[2] U.L. Andersen, G. Leuchs, C. Silberhorn, Continuous-variable quantum information processing, Laser Photonics Rev. 4 (2010) 337.

[3] J.N. Bandyopadhyay, A. Lakshminarayan, Testing statistical bounds on entanglement using quantum chaos, Phys. Rev. Lett. 89 (2002) 060402.

[4] J.N. Bandyopadhyay, A. Lakshminarayan, Entanglement production in coupled chaotic systems: case of the kicked tops, Phys. Rev. E 69 (2004) 016201.

[5] M.V. Berry, Quantum scars of classical closed orbits in phase space, Proc. R. Soc. Lond. A 423 (1989) 219–231.

[6] S.L. Braunstein, P. van Loock, Quantum information with continuous variables, Rev. Mod. Phys. 77 (2003) 513.

[7] G. Casati, I. Guarneri, J. Reslen, Classical dynamics of quantum entanglement, Phys. Rev. E 85 (2012) 036208.

[8] S. Chaudhury, A. Smith, B.E. Anderson, S. Ghose, P.S. Jessen, Quantum sigs of chaos in a kicked top, Nature 461 (2009) 768–771.

[9] N.N. Chung, L.Y. Chew, Energy eigenvalues and squeezing properties of general systems of coupled quantum anharmonic oscillators, Phys. Rev. A 76 (2007) 032113.

[10] N.N. Chung, L.Y. Chew, Dependence of entanglement dynamics on the global classical dynamical regime, Phys. Rev. E 80 (2009) 016204.

[11] N.N. Chung, L.Y. Chew, Two-step approach to the dynamics of coupled anharmonic oscillators, Phys. Rev. A 80 (2009) 012103.

[12] J. Emerson, Y.S. Weinstein, S. Lloyd, D.G. Cory, Fidelity decay as an efficient indicator of quantum chaos, Phys. Rev. Lett. 89 (2002) 284102.

[13] C.H. Er, N.N. Chung, L.Y. Chew, Threshold effect and entanglement enhancement through local squeezing of initial separable states in continuous-variable systems, Phys. Scr. 87 (2013) 025001.

[14] H. Fujisaki, T. Miyadera, A. Tanaka, Dynamical aspects of quantum entanglement for weakly coupled kicked tops, Phys. Rev. E 67 (2003) 066201.

[15] F. Furrer, T. Franz, M. Berta, A. Leverrier, V. Scholz, M. Tomamichel, R. Werner, Continuous variable quantum key distribution: finite-key analysis of composable security against coherent attacks, Phys. Rev. Lett. 109 (2012) 100502.

[16] S. Furuichi, A.A. Mahmoud, Entanglement in a squeezed two-level atom, J. Phys. A, Math. Gen. 34 (2001) 6851.

[17] K. Furuya, M.C. Nemes, G.Q. Pellegrino, Quantum dynamical manifestation of chaotic behavior in the process of entanglement, Phys. Rev. Lett. 80 (1998) 5524–5527.

[18] F. Galve, L.A. Pachón, D. Zueco, Bringing entanglement to the high temperature limit, Phys. Rev. Lett. 105 (2010) 180501.

[19] S. Ghose, B.C. Sanders, Entanglement dynamics in chaotic systems, Phys. Rev. A 70 (2004) 062315.

[20] M. Gutzwiller, Chaos in Classical and Quantum Mechanics, Interdisciplinary Applied Mathematics, Springer-Verlag, 1990.

[21] F. Haake, K. Życzkowski, Random-matrix theory and eigenmodes of dynamical systems, Phys. Rev. A 42 (1990) 1013–1016.

[22] S. Heusler, S. Müller, A. Altland, P. Braun, F. Haake, Periodic-orbit theory of level correlations, Phys. Rev. Lett. 98 (2007) 044103.

[23] X.W. Hou, J.H. Chen, B. Hu, Entanglement and bifurcation in the integrable dimer, Phys. Rev. A 71 (2005) 034302.

[24] X.W. Hou, J.H. Chen, Z.Q. Ma, Dynamical entanglement of vibrations in an algebraic model, Phys. Rev. A 74 (2006) 062513.

[25] A. Kowalewska-Kudłaszyk, J. Kalaga, W. Leoński, Long-time fidelity and chaos for a kicked nonlinear oscillator system, Phys. Lett. A 373 (2009) 1334–1340.

[26] A. Kowalewska-Kudłaszyk, J. Kalaga, W. Leoński, V.C. Long, Kullback–Leibler quantum divergence as an indicator of quantum chaos, Phys. Lett. A 376 (2012) 1280–1286.

[27] M. Kus, J. Mostowski, F. Haake, Universality of eigenvector statistics of kicked tops of different symmetries, J. Phys. A, Math. Gen. 21 (1988) L1073.

[28] A. Lakshminarayan, Entangling power of quantized chaotic systems, Phys. Rev. E 64 (2001) 036207.

[29] S.B. Lee, M.D. Feit, Signatures of quantum chaos in Wigner and Husimi representations, Phys. Rev. E 47 (1993) 4552–4555.

[30] M. Lombardi, A. Matzkin, Dynamical entanglement and chaos: the case of Rydberg molecules, Phys. Rev. A 73 (2006) 062335.

[31] M. Lombardi, A. Matzkin, Entanglement and chaos in the kicked top, Phys. Rev. E 83 (2011) 016207.

[32] P. van Loock, S. Braunstein, Unconditional teleportation of continuous-variable entanglement, Phys. Rev. Lett. 87 (2001) 247901.

[33] A. Matzkin, M. Raoult, D. Gauyacq, Observation of diffractive orbits in the spectrum of excited no in a magnetic field, Phys. Rev. A 68 (2003) 061401.

[34] P.A. Miller, S. Sarkar, Signatures of chaos in the entanglement of two coupled quantum kicked tops, Phys. Rev. E 60 (1999) 1542–1550.

[35] M. Novaes, Entanglement dynamics for two interacting spins, Ann. Phys. 318 (2005) 308–315.

[36] A. Peres, Stability of quantum motion in chaotic and regular systems, Phys. Rev. A 30 (1984) 1610–1615.

[37] R.A. Pullen, A.R. Edmonds, Comparison of classical and quantum spectra for a totally bound potential, J. Phys. A, Math. Gen. 14 (1981) L477.

[38] M. Reid, P. Drummond, Quantum correlations of phase in nondegenerate parametric oscillation, Phys. Rev. Lett. 60 (1988) 2731.

[39] A. Shahinyan, L.Y. Chew, G. Kryuchkyan, Probing quantum dissipative chaos using purity, Phys. Lett. A 377 (2013) 2743–2748.

[40] B. Shao, S. Xiang, K. Song, Quantum entanglement and nonlocality properties of two-mode gaussian squeezed states, Chin. Phys. B 18 (2009) 418.

[41] L. Song, X. Wang, D. Yan, Z. Zong, Entanglement dynamics and chaos in the Dicke model, Int. J. Theor. Phys. 47 (2008) 2635–2644.

[42] M. Tomiya, N. Yoshinaga, S. Sakamoto, A. Hirai, A large number of higher-energy eigenvalues of a huge dimensional matrix for a quantum chaotic study of a quartic potential, Comput. Phys. Commun. 169 (2005) 313–316.

[43] X. Wang, S. Ghose, B.C. Sanders, B. Hu, Entanglement as a signature of quantum chaos, Phys. Rev. E 70 (2004) 016217.

[44] C. Weedbrook, S. Pirandola, R. Garcia-Patron, N.J. Cerf, T.C. Ralph, J.H. Shapiro, S. Lloyd, Gaussian quantum information, Rev. Mod. Phys. 84 (2012) 621.

[45] L.J. Zhai, Y.J. Zheng, S.L. Ding, Vibrational chaotic dynamics in triatomic molecules: a comparative study, Front. Phys. 7 (2012) 514.

[46] S.H. Zhang, Q.L. Jie, Quantum-classical correspondence in entanglement production: entropy and classical tori, Phys. Rev. A 77 (2008) 012312.

[47] Y. Zhang, H. Wang, X. Li, J. Jing, C. Xie, K. Peng, Experimental generation of bright two-mode quadrature squeezed light from a narrow-band nondegenerate optical parametric amplifier, Phys. Rev. A 62 (2000) 023813.